On the Use of a Hybrid Approach to Contrast Endmember Induction Algorithms

Miguel A. Veganzones and Carmen Hernández

Computational Intelligence Group, UPV/EHU
Facultad Informatica, Paseo Manuel de Lardizabal
San Sebastian, Spain
www.ehu.es/ccwintco

Abstract. In remote sensing hyperspectral image processing, identifying the constituent spectra (endmembers) of the materials in the image is a key procedure for further analysis. The contrast between Endmember Inductions Algorithms (EIAs) is a delicate issue, because there is a shortage of validation images with accurate ground truth information, and the induced endmembers may not correspond to any know material, because of illumination and atmospheric effects. In this paper we propose a hybrid validation method, composed on a simulation module which generates the validation images from stochastic models and evaluates the EIA through Content Based Image Retrieval (CBIR) on the database of simulated hyperspectral images. We demonstrate the approach with two EIA selected from the literature.

1 Introduction

The high spectral resolution provided by current hyperspectral imaging devices facilitates identification of fundamental materials that make up a remotely sensed scene [1, 6]. In the field of hyperspectral image processing, identify the constituent spectra (endmember) of the materials in the image is a key procedure for further analysis, i.e., unmixing, thematic map building, target detection, unsupervised segmentation. A library of known pure ground image spectra or laboratory sample spectra could be used. However, this poses several problems, such as the effects of the illumination on the observed spectra, the difference in sensor intrinsic parameters and the *a priori* knowledge about the material composition of the scene. Besides the methodological questions, this approach is not feasible when trying to process large quantities of image data. Current approaches try to induce automatically the endmembers from the image data itself, the so called Endmember Induction Algorithms (EIA). They try either to select some image pixel spectra as the best approximation to the endmembers in the image (i.e. [4]), or to compute estimations of the endmembers on the basis of the transformations of the image data (i.e. [5, 10]).

The comparison among the relative performances of these algorithms is a delicate issue. In essence, these algorithms are unsupervised: they explore the data or transformations of the unlabeled data. Therefore, validation approaches based on the quality of some classification performance measure may be inaccurate. Besides, there are big difficulties in obtaining good quality labeled hyperspectral test images. In this work

we propose a hybrid approach for validation. The first part of the approach is a hyperspectral image simulation module based on random field generation approaches. This module is used to generate the test images, with known endmembers and realistic abundance spatial distribution ground truth, that will be used for the comparison between algorithms. The second part of the approach consists of a Content Based Image Retrieval (CBIR) [9, 3] scheme based on a distance defined on the set of endmembers induced from the image. We do not impose classification like schemes as the performance measures, but we evaluate the ability of the algorithms to uncover the underlying mixtures. We apply this methodology to compare the Endmember induction Heuristic Algorithm (EIHA) [4], with respect to the well known geometrical algorithm N-FINDER [10].

The structure of the paper is as follows: In section 2 we detail the proposed EIAs contrast methodology based on CBIR systems. Section 3 gives a short review of the the algorithms compared in this demonstration of the approach. In section 4 we define the experiments and present the results. Finally, we give some conclusions in section 5.

2 Contrast of EIAs Based on CBIR

In this section we will first describe the details of the simulation module that provides the test images, then we present the similarity measure between hyperspectral images and finally we describe the comparison methodology as a whole.

2.1 Synthetic Hyperspectral Image Module

The hyperspectral images used for the algorithm contrast are generated as linear mixtures of a set of spectra (the ground-truth endmembers) with synthesized abundance images. The ground-truth endmembers were randomly selected from a subset of the USGS spectral library.

The synthetic ground-truth abundance images were generated in a two-step procedure. First, we simulate each abundance as a gaussian random field with Matern correlation function of parameters $\theta_1 = 10$ and $\theta_2 = 1$. We applied the procedure proposed by [7] for the efficient generation of a big domain of gaussian random fields. Second, to ensure that there are regions of almost pure endmembers, we selected for each pixel the abundance coefficient with the greatest value and we normalize the remaining coefficients to ensure that the normalized abundance coefficients sum up to one. It can be appreciated on the abundance images that each endmember has several regions of almost pure pixels, viewed as brighter regions in the images.

We have synthesized a total of 6000 hyperspectral images divided in three datasets of 2000 images each. Each dataset is defined by the number of endmembers in the repository of ground-truth endmembers. We defined three repositories of ground-truth endmembers with 5, 10 and 20 endmembers each, representing an increasing diversity in the materials present in the dataset. The size of the images is 256x256 pixels with 269 spectral bands each. For each dataset we have generated collections of 500 images by the following procedure:

– First, we randomly decide the number of endmembers in the image, between 2 and 5.

– Second, we select the image ground-truth endmembers from the corresponding repository of ground-truth endmembers.
– Third, we generate the synthetic abundance images corresponding to each endmember, applying the corrections commented before.

Figure 1 shows a subset of the collection of ground-truth endmembers. Figure 2 shows an example of the selected endmembers and the generated images of abundances to synthesize an hyperspectral image.

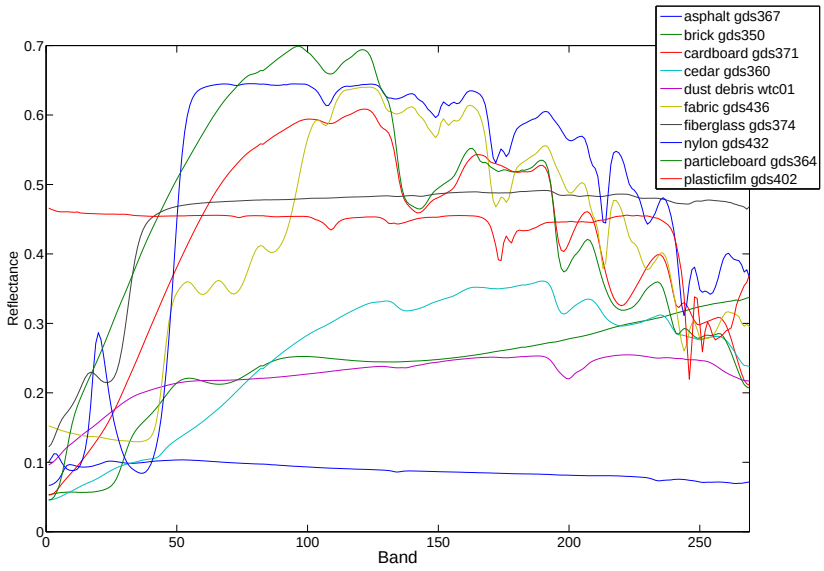

Fig. 1. Subset of endmembers selected from the USGS library to synthesize the hyperspectral images datasets.

2.2 Dissimilarity Between Hyperspectral Images

A CBIR system is based on the definition of a similarity measure between the images. For hyperspectral images, two kind of informations can be used to build such a dissimilarity measure: the spectral and the spatial informations. Because we are interested in exploiting the spectral information, each hyperspectral image H is characterized by a set of induced endmembers E. A dissimilarity measure between two hyperspectral images, $S\left(H_\xi, H_\gamma\right)$, is defined in terms of the distances between their corresponding sets of endmembers.

Let it be $E_\xi = \left\{\mathbf{e}_1^\xi, \mathbf{e}_2^\xi, \ldots, \mathbf{e}_{p_\xi}^\xi\right\}$ the set of endmembers induced from the image H_ξ in the database, where p_ξ is the number of induced endmembers from the ξ-th image. Given two images, H_ξ, H_γ, we compute the following matrix whose elements

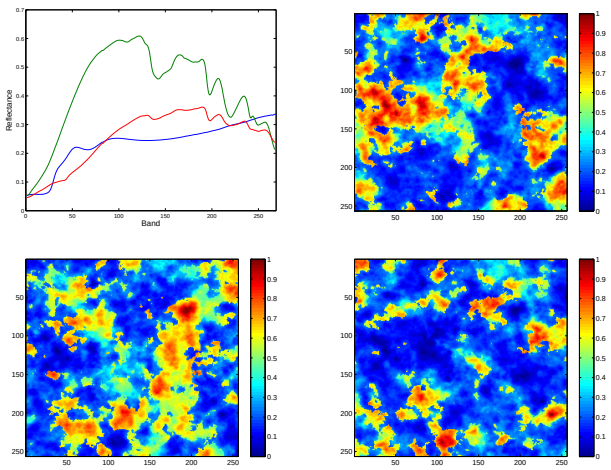

Fig. 2. Example of the endmembers and abundance images used to generate a synthetic hyperspectral image. This example corresponds to a 10-endmembers dataset image using 3 endmembers.

are the distances between the pairs of endmembers built as all the possible combination of endmember from each image:

$$D_{\xi,\gamma} = [d_{i,j};\ i = 1,\ldots,p_\xi;\ j = 1,\ldots,p_\gamma]\,, \tag{1}$$

where $d_{i,j}$ is any defined distance between the endmembers $\mathbf{e}_i^\xi$ and $\mathbf{e}_j^\gamma$, i.e. the Euclidean distance, $d_{i,j} = \left\|\mathbf{e}_i^\xi - \mathbf{e}_j^\gamma\right\|^2$. Then the dissimilarity between the images is given as a function of the distance matrix (1) by the following equation:

$$S\left(H_\xi, H_\gamma\right) = \left(\|\mathbf{m}_r\| + \|\mathbf{m}_c\|\right)\left(|p_\xi - p_\gamma| + 1\right), \tag{2}$$

where $\mathbf{m}_r$ and $\mathbf{m}_c$ are the vectors built of the minimal values of the distance matrix, $D_{\xi,\gamma}$, computed across rows and columns respectively. That is, the elements of the the row vector of minima are computed as follows:

$$m_{r,i} = \min_j \left\{d_{ij}\right\};\ i = 1,\ldots,p_\xi.$$

Note that the endmember induction algorithm can give different number of endmembers for each image. The proposed dissimilarity function can cope with this asymmetry avoiding the combinatorial problem of trying to decide which endmembers can be matched and what to do in case that the number of endmembers is different from one image to the other.

2.3 Methodology for the Contrast of EIAs

We propose here the summary methodology for the comparison among EIAs which hybridizes hyperspectral image simulation and CBIR performance measurements. The CBIR approach is based on the dissimilarity measure (2) presented in the previous section. The comparison methodology consists on the following steps:

1. Build a database of synthetic hyperspectral images using a set of ground truth endmembers and simulated abundance images.
2. Compute the dissimilarity between each image pair in the database on the basis of the image ground truth endmembers. For each image rank the remaining images in the database with respect to their *ground truth* dissimilarity to it.
3. For each image in the dataset compute its endmembers using the EIAs. We will obtain as many endmember sets per image as EIAs are to be compared.
4. Compute the dissimilarity between each image pair in the database on the basis of the induced endmembers. For each image rank the remaining images in the database with respect to their *induced* dissimilarity to it.
5. Compare the rankings obtained by the use of ground truth endmembers and induced endmembers.

First step involves the generation of in-lab controlled hyperspectral datasets. Although the ground-truth endmembers used to generate the synthetic images are going to be used to validate the EIA performance, we are not interested in compare them directly with the induced endmembers. The induced endmembers could have great differences respect to the real ones, but still they could retain enough discriminative information for the problem we are trying to solve, being of high relevance.

Second step computes the dissimilarity measures between each image in the dataset using the ground-truth endmembers. This provide us the expected results for a given query, and so, the point of reference to define the performance measures.

Third step makes use of an EIA to induce the endmembers from each image in the dataset. In the fourth step, those induced endmembers will be used to obtain the disimilarites between each image in the dataset, using the same dissimilarity function than in the step two. In figure 3 we illustrate how the dissimilarity ranking can vary when computed on the ground truth endmembers (blue line) or the induced endmembers (red line). An error measure of the induced endmembers could be the area between both lines, however we are not interested in such kind of measures, we prefer a more qualitative evaluation in terms of the recalling power of the CBIR system built over the above dissimilarity measure.

From a CBIR point of view, the objective is to retrieve the k more similar images from a dataset given a query image. This methodology compares the results of a set of queries using the induced endmembers to the results using the ground-truth endmembers. This would indicate the ability of the used EIA to retrieve spectral information relevant for CBIR purposes. Step five use precision and recall measures to compare the EIAs on the basis of CBIR performance. Precision is defined as the fraction of the retrieved images that are relevant to the query, and recall as the fraction of the total number of relevant images (contained in the archive) that are retrieved [2]: $precision_K = \frac{|R \cap T|}{|T|}$ and $recall_K = \frac{|R \cap T|}{|R|}$, where T is the set of returned images and R is the set of images relevant to the query of size K.

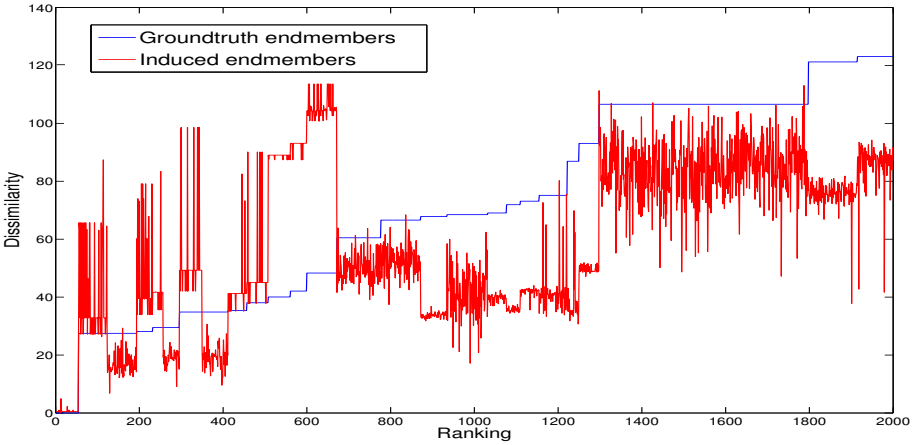

Fig. 3. Dissimilarity respect to one image in the database, based on ground truth endmembers (blue line) and based on induced endmembers (red line). Images are ordered according to increasing ground truth dissimilarity.

3 Endmember Induction Algorithms

Following the definition of the linear mixing model [6], the hyperspectral images are defined as the result of the linear combination of the pure spectral signature of ground components, so-called endmembers. Let $\mathbf{E} = [\mathbf{e_1}, \ldots, \mathbf{e_p}]$ be the pure endmember signatures (normally corresponding to macroscopic objects in scene, such as water, soil, vegetation, ...) where each $\mathbf{e_i} \in \mathbb{R}^L$ is an L-dimensional vector. Then, the hyperspectral signature $\mathbf{r}$ at each pixel on the image is defined by the expression: $\mathbf{r} = \sum_{i=1}^{p} \mathbf{e_i}\phi_i + \mathbf{n}$, where the hyperspectral signature $\mathbf{r}$ is formed by the sum of the fractional contributions of each endmember and an independent additive noise component $\mathbf{n}$. ϕ is the p-dimensional vector of fractional abundances at a given pixel . This equation can be extended to the full image as follows: $\mathbf{H} = \mathbf{E\Phi} + \mathbf{n}$, where $\mathbf{H}$ is the hyperspectral image and $\mathbf{\Phi}$ is a matrix of fractional abundances. Therefore, the linear mixing model assumes that the endmembers are the vertices of a convex set that covers the image data. Because the distribution of the data in the hyperspace is usually tear-shaped most of the geometrical EIAs look for the minimum simplex that covers all the data.

The N-FINDER [10] is one of the algorithms following this approach. It works by inflating a simplex inside the data, beginning with a random set of pixels. Previously, data dimensionality has to be reduced to $n-1$ dimensions, being n the number of endmembers searched for. The algorithm starts by selecting an initial random set of pixels as endmembers. Then for each pixel and each endmember, the endmember is replaced with the spectrum of the pixel and the volume recalculated. If the volume increases, the endmember is replaced by the spectrum of the pixel. The procedure ends when no more replacements are done. The algorithm needs of some random initializations to avoid local maxima.

The second algorithm tested is Endmember Induction Algorithm (EIHA) was fully described in [4], so that here we will only recall some of its main features. The algorithm is based on the equivalence between Strong Lattice Independence and Affine Independence [8]. Strong Lattice Independence is a concept born in the field of Morphological Associative Memories, which became the field of Lattice Associative Memories. A set of vectors is said to be Lattice Independent if no one of them is a Linear Minimax combination of the remaining ones. It is Strong Lattice Independent if moreover there is min or max dominance defined on the set. One way to find sets of Strong Lattice Independent vectors is to progressively build Lattice Auto-Associative Memories (LAAM) with the detected endmembers. Because of the convergence properties of the Lattice Auto-Associative Memories, lattice dependent vectors will be recall-invariant, so lattice independent vectors can be detected as non-recall-invariant vectors. The EIHA proposed in [4] includes a noise filter that discards candidate vectors which are too close to the already detected endmembers.

4 Experimental Results

Figure 4 shows the $precision_k(H)$ and $recall_k(H)$ results of the N-FINDER and EIHA (denoted LAM in the figures) algorithms respect to three defined synthetic hyperspectral image databases, generated from a collection of 10 basic endmembers selected from the USGS library of spectral signatures, for all possible values of the size of the response K using the dissimilarity function 2. It can be appreciated that the behavior of both algorithms is quite similar. The recall is very low when the size of ground truth repository is 5, increases with the repository size, meaning that a greater variety of ground truth endmembers improves the probability of recalling relevant images. Contrary to that, the precision is greater for the smaller repository, and increasing the repository size decreases the precision of the responses. The precision of the EIHA in always better for small query size and for very big query sizes. There is some intermediate query size region where the precision of N-FINDER improves that of EIHA. Overall, both algorithms performance is comparable, and the selection of the most appropriate depends on the application setting. The query size may be the criterion for the selection.

5 Conclusions

We propose a hybrid approach for the evaluation and comparison of Endmember Induction Algorithms (EIA). First a simulation module generates tailored databases of realistic hyperspectral images. Instead of the conventional classification performances we propose the use of CBIR based performance measures, where the CBIR is based on the spectral information of the images, that is, the dissimilarity between images is computed based on the distances between the sets of endmembers that characterize spectrally the image. We have show some results comparing two EIA from the literature. This comparison allows to identify some problem dependent parameters that would justify the selection of one algorithm over the other: query size, ground truth endmember variety. Further work may be addressed to test new EIA in this framework.

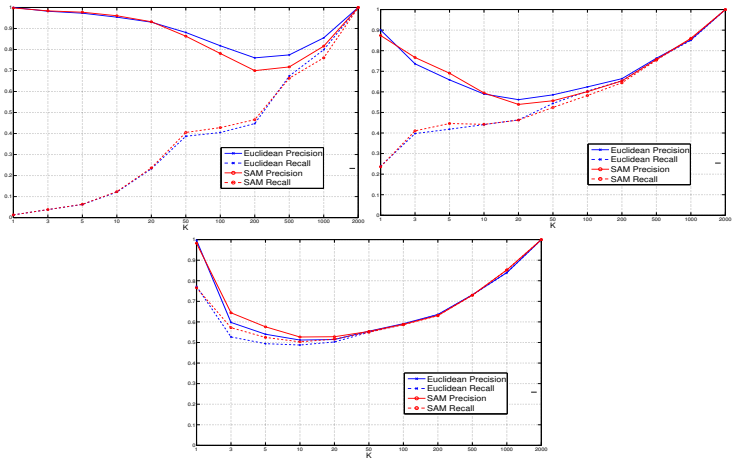

Fig. 4. Precision and recall results for each dataset: (a) 5 endmembers dataset (b) 10 endmembers dataset (c) 20 endmembers dataset

References

1. Roger N. Clark and Ted L. Roush. Reflectance spectroscopy: Quantitative analysis techniques for remote sensing applications. *Journal of Geophysics Research*, 89(B7):6329–6340, 1984.
2. H. Daschiel and M. Datcu. Information mining in remote sensing image archives: system evaluation. *Geoscience and Remote Sensing, IEEE Transactions on*, 43(1):188–199, 2005.
3. M. Datcu and K. Seidel. Human centered concepts for exploration and understanding of satellite images. In *Advances in Techniques for Analysis of Remotely Sensed Data, 2003 IEEE Workshop on*, pages 52–59, 2003.
4. M. Grana, I. Villaverde, J. O. Maldonado, and C. Hernandez. Two lattice computing approaches for the unsupervised segmentation of hyperspectral images. *Neurocomputing*, 72:2111–2120, 2009.
5. A. Ifarraguerri and C. -I Chang. Multispectral and hyperspectral image analysis with convex cones. *Geoscience and Remote Sensing, IEEE Transactions on*, 37(2):756–770, 1999.
6. N. Keshava and J. F Mustard. Spectral unmixing. *Signal Processing Magazine, IEEE*, 19(1):44–57, 2002.
7. Boris Kozintsev. *Computations with Gaussian Random Fields, PhD Thesis*. University of Maryland, 1999.
8. G. X. Ritter and P. Gader. Fixed points of lattice transforms and lattice associative memories. In *Advances in imaging and electron physics*, number 143 in Advances in imaging and electron physics, page 264. Academic press, 2006.
9. A.W.M. Smeulders, M. Worring, S. Santini, A. Gupta, and R. Jain. Content-based image retrieval at the end of the early years. *Pattern Analysis and Machine Intelligence, IEEE Transactions on*, 22(12):1349–1380, 2000.
10. M. E Winter, M. R Descour, and S. S Shen. N-FINDR: an algorithm for fast autonomous spectral end-member determination in hyperspectral data. volume 3753, pages 266–275, Denver, CO, USA, October 1999. SPIE.